Journal of King Saud University – Engineering Sciences (2025) 37:44
https://doi.org/10.1007/s44444-025-00049-z

ORIGINAL PAPER

Electro-induced two-way shape memory effect from novel interpenetrating polymer networks based on poly(benzoxazine/urethane) reinforced with carbon fiber felt

Kittipon Bunyanuwat[1] · Phattarin Mora[2] · Panuwat Luengrojanakul[1] · Chaweewan Sapcharoenkun[3] · Jinying Yuan[4] · Panagiotis Karagiannidis[5] · Sarawut Rimdusit[1]

Received: 17 April 2025 / Accepted: 7 September 2025

Abstract

Novel two-way shape memory polymer composites (2WSMPC) consisting of interpenetrating polymer networks (IPNs) of poly(benzoxazine/urethane) reinforced with carbon fiber felt (CFF) were developed in this work. Sequential curing, i.e., moisture curing of urethane followed by thermal curing of benzoxazine (BA-a) was used to synthesize IPNs with molecular phase separation. The thermomechanical properties and two-way shape memory effect (2WSME) of the IPNs were systematically investigated by varying the urethane content. It was found that the glass transition temperature (T_g) and 2WSME of the IPNs based on poly(benzoxazine/urethane) improved by optimizing the urethane content. Moreover, the electro-induced shape memory performance was found to be dependent on the CFF reinforcement. The results showed that the developed IPNs reinforced with CFF triggered by electric current exhibited high two-way shape memory performance, i.e., a fixity at room temperature (RT) of 97–98%, recovery to original shape at high temperature of 97–98%, and those to temporary shape at RT of 92–97%. The findings revealed that the electro-induced two-way shape memory composite from CFF-reinforced poly(benzoxazine/urethane) is a promising candidate for smart electric circuit breaker applications with highly stable reverse recovery between original and temporary shapes up to 20 cycles.

Keywords Two-way shape memory composites · Benzoxazine · Urethane · Carbon fiber felt · Interpenetrating polymer networks

1 Introduction

Shape memory materials (SMMs), shape memory polymers (SMPs), and shape memory polymer composites (SMPCs) are smart materials which respond to external stimuli by transitioning between a temporary configuration and their original shape (Goyal et al. 2021; Rouf et al. 2022; Xia et al. 2021; Zeng et al. 2023). The SMPs are categorized into one-way SMPs (1WSMPs) and two-way SMPs (2WSMPs) based on the mechanism by which they revert to their original shape. 1WSMPs are non-reversible shape-shifting; i.e., when applying a reverse stimulus, the temporary shape is unrecoverable to the original shape. On the contrary, 2WSMPs are cyclically reversible between two shape-shifting phases when triggered by a reverse stimulus. Consequently, 2WSMPs have recently received interest due to their applicability in a wide range of applications (Lee et al. 2017; Ruenpanya et al. 2024; Zare et al. 2019).

✉ Sarawut Rimdusit
sarawut.r@chula.ac.th

1 Center of Excellence in Polymeric Materials for Medical Practice Devices, Department of Chemical Engineering, Faculty of Engineering, Chulalongkorn University, Bangkok 10330, Thailand

2 Department of Chemical Engineering, Faculty of Engineering, Srinakharinwirot University, Nakhonnayok 26120, Thailand

3 National Nanotechnology Center (NANOTEC), National Science and Technology Development Agency (NSTDA), Thailand Science Park, Phahonyothin Rd., Khlong Nueng, Khlong Luang 12120, Pathumthani, Thailand

4 Key Lab of Organic Optoelectronics and Molecular Engineering of Ministry of Education, Department of Chemistry, Tsinghua University, Beijing 100084, China

5 School of Computer Science and Engineering, Faculty of Business and Technology, University of Sunderland, Sunderland SR6 0DD, UK

Published online: 03 November 2025

Over the decades, SMPs derived from polybenzoxazine received attention due to their versatility of copolymerization by their inherent phenolic hydroxyl groups with other polymer systems (Ishida & Agag 2011; Rimdusit et al. 2013), such as epoxy resin (Amornkitbamrung et al. 2022; Tanpitaksit 2015), polycaprolactone (PCL) (Schäfer et al. 2018, 2019), and urethane (Gu & Jana 2014; Jamnongpak et al. 2024). Furthermore, no volatile by-products are released upon curing of benzoxazine, unlike traditional phenolic resins (Ishida & Allen 1996). Herein, polybenzoxazine usually plays an important role as a stable network segment, providing improved thermal stability to the polymer system and enhancing the SMP performance in terms of fixity. Prathumrat et al. (2017b) developed a one-way multiple-SMP based on benzoxazine/urethane prepolymer (BA-a/UP) alloys, which could be formed into two different temporary shapes determined by their broad T_g range. Mora et al. (2023) developed two-way thermo-responsive SMPs based on BA-a/UP alloys obtained from conventional thermal curing. Their investigations revealed that the gradient heterogeneous networks of PU-rich domains and BA-a/UP network resulted in an improvement of 2WSMP performance. However, 2WSMPs fabricated from the alloys with gradient heterogeneous networks have the Limitations of one-side shape memory deformation and irreversibility between the original and one of the temporary shapes. Thus, to overcome these problems, 2WSMPs having molecular phase separation need to be developed.

2WSMPs exhibit reversible and programmable morphological transformations, governed by variations in molecular phase separation behavior, i.e. (Zare et al. 2019) liquid crystalline elastomers (LCEs) (Ohm et al. 2010; Yang et al. 2022), shape memory composites or laminates (SMC) (Chen et al. 2015; Leng et al. 2011), and interpenetrating polymer networks (IPN) (Ratna & Karger-Kocsis 2011; Wu et al. 2014b) (Li et al. 2011; Zhou et al. 2014). Yang et al. (2022) reported 2WSMPs from a double-block polyurethane (PU) cross-linked network between hydroxy-terminated poly(*L*-lactic acid) (PLA) and hydroxy-terminated poly(ε-caprolactone) (PCL) with PU. Their findings indicated that the copolymer exhibits two distinct melting temperatures, associated with the PLA as the rigid part and PCL with PU as the flexible part. Referring to previous research, in IPNs of epoxy/PU and in LCEs of polylactic acid/caprolactone, the PU was the flexible segment in 1WSMP and 2WSMPs. Based on the mentioned studies, it can be concluded that polyurethanes are one of the promising flexible segment candidates for the development of SMPs.

The external stimulus for 2WSMPs is typically direct or indirect heat actuated by various stimuli, i.e., electric current (Arun et al. 2019; Yao et al. 2016), magnetic field (Phetnoi et al. 2024; Ruenpanya et al. 2024), and light (Amornkitbamrung et al. 2020; Leungpuangkaew et al. 2023). However, the stimulus of direct heating comes with limitations; the system has to be in close proximity with the heat source and is dependent on an external heater, which can sometimes be unfeasible, troublesome, or even hazardous for some applications (Sánchez et al. 2022). Indirect heating may be preferred over direct heating, as it overcomes these limitations. One of the most effective indirect heating stimuli is electric current due to its faster response times and reversible actuation compared to that of direct heating, allowing for more dynamic and rapid shape changes (Qi et al. 2016; Sánchez et al. 2022; Shao et al. 2015). Consequently, electro-active SMPs, which were triggered by electric current, were used instead of thermo-active SMPs in various applications such as 4D printing (Huang et al. 2021), soft robotics (Maksimkin et al. 2022), aerospace (Singh et al. 2022; Zhou et al. 2023), smart electronic devices (Wang et al. 2016), and biomedical devices (Li et al. 2019; Pringpromsuk et al. 2020). Nevertheless, the SMPs actuated by electric current suffer from low thermal and electrical conductivity. Electro-induced SMPCs reinforced with conductive fillers, such as particles or fibers, are one of the best strategies to improve the electrothermal actuation properties of SMPs (Leng et al. 2007; Tang et al. 2013).

Recently, carbon fiber felt (CFF) was used to reinforce SMP systems aimed to be an alternative stimulus for electronic device applications (Gong et al. 2016). Gong et al. (2016) developed SMPCs using CFF to reinforce epoxy resin. The advantage of CFF is that it serves as an excellent conductive filler that readily disperses throughout the composite; it is low cost, and it is easily produced. Results revealed the display of the recovery effect in the SMPC triggered by electric current via Joule heating.

Therefore, in the present work, 2WSMP from IPNs based on poly(benzoxazine/urethane) were prepared by sequential curing. The effect of PU incorporation on the thermomechanical properties and 2WSMP properties of poly(benzoxazine/urethane) was investigated. To further develop the electro-induced two-way shape memory effect of the IPNs, the influence of CFF reinforcement as a conductive filler into the IPNs on the essential properties was also studied. In addition, electro-induced SMPCs reinforced with CFF were also prepared to study the electro-induced shape memory performance for the electric circuit breaker application.

2 Experimental section

2.1 Materials

Bisphenol-A (polycarbonate grade), paraformaldehyde (AR grade), and aniline (AR grade) were purchased from PTT Phenol Co., Ltd. (Thailand), Merck Co., Ltd. (Darmstadt,

Germany), and Loba Chemie Pvt. Ltd. (Mumbai, India), respectively. 2,4-Tolylene diisocyanate (2,4-TDI) and polypropylene glycol (PPG) (MW 2000 Da) were obtained from TCI Chemicals (Tokyo, Japan) and Sigma-Aldrich Pte. Ltd. (Singapore), respectively. The CFF (30 gsm) was purchased from Future Fiber Ltd. (Thailand), composed of non-woven randomly oriented carbon fibers. All chemicals and fibers were used as received.

2.2 Synthesis of benzoxazine resin and urethane prepolymer

Bisphenol-A aniline-based benzoxazine resin (BA-a) was prepared by a melt condensation reaction of bisphenol-A, paraformaldehyde, and aniline at a molar ratio of 1:4:2 via solventless technology (Ishida 1996). The reactants were blended together at 110 °C for 40 min to yield a transparent vitreous yellow product at RT. Urethane prepolymer (UP) was synthesized by reacting 2,4-TDI with PPG at 80 °C for 2 h in a four-neck round-bottom flask under constant agitation and nitrogen (N_2) purge. The obtained UP was a transparent viscous liquid, which was then cooled down to RT, stored in a N_2-purged container, and kept in a refrigerator for later use.

2.3 Fabrication of poly(benzoxazine/urethane) via sequential curing

The BA-a resin and UP were mixed together thoroughly in a silicone mold at 110 °C at various mass ratios of 90:10, 80:20, 70:30, and 60:40 until a homogenous mixture was obtained, followed by cooling down to RT. The resultant mixture was then first Kept in a desiccator and conditioned at a relative humidity of 90% for 48 h to allow the PU to completely achieve network formation. After that, the binary mixtures were thermally cured in an air-circulated oven using a step heating profile of 150 °C for 1 h, 170 °C for 1 h, 190 °C for 2 h, and 200 °C for 1 h to polymerize the benzoxazine network.

2.4 Sample characterization

Fourier transform infrared (FTIR) spectroscopy (Perkin Elmer Spectrum GX FTIR spectrometer with an ATR) was used to investigate the moisture curing of BA-a/UP mixtures. All spectra were recorded using 64 scans in the spectral range of 4000–650 $cm^{-1}$and resolution of 4 cm^{-1}.

A differential scanning calorimeter (DSC) (model DSC1, Mettler Toledo, Greifensee, Switzerland) was used to study the thermal curing of the binary mixtures. The tests were conducted from 30 to 300 °C by a heating ramp rate of 10 °C/min under N_2 atmosphere (50 mL/min flow rate).

A dynamic mechanical analyzer (DMA) (model DMA 1, Mettler Toledo, Greifensee, Switzerland) was used to determine the thermomechanical properties in a dual-cantilever mode under an air atmosphere. The dimensions of the specimen were $10 \times 50 \times 2$ mm^3. The tests were performed at a fixed frequency of 1 Hz and a heating rate of 2 °C/min from − 100 up to 300 °C. The peak of the loss tangent curves was taken as T_g. The storage modulus (E′) at the glassy state of the specimens was also examined.

The phase morphology of specimens was characterized by atomic force microscopy (AFM) at RT by using a NanoWizard3 atomic force microscope from JPK Instruments (Germany). The force spectroscopic mapping QI (quantitative imaging) mode was used. In this mode, a force-distance spectrum is taken at each pixel in the scanned surface area, and these are used to create adhesion force images. The probe tip was compressed into the scanned points with a loading force of around 100 nN, pixel time of 14 ms, and a vertical distance of 1000 nm. Image processing was performed using the DP software supplied with the JPK AFM system.

A scanning electron microscope (SEM, model JSM-6510A from JEOL Ltd., Tokyo Japan) was used to observe the morphology of the specimens at 15 kV acceleration voltage. A thin gold layer was primarily applied on all specimens by using a JEOL ion sputtering device (model JFC-1200).

The shape memory properties of the specimens with dimensions of $50 \times 5 \times 0.5$ mm^3 were determined under stimuli. The 2WSMP programming was set up as shown in Fig. 1a–c under direct heating trigger. The original specimen was heated up to $T_g + 20$ °C and maintained at that temperature for 5 min without any loading. Then, the specimen was cooled down to RT while constantly applying bending load until reaching the intended fixation angle of 130° to fix a temporary shape. The 2WSMP recovery was performed as demonstrated in Fig. 1d–f. The temporary shape of the specimen was directly heated or indirectly heated by electric current to $T_g + 20$ °C to convert its shape to the original state (intended angle of 180°). After that, the specimen automatically recovered to its temporary shape once it was cooled down to RT. 2WSMP specimen would be obtained with reversibility between original and temporary shapes. Notably, the shape memory programming conditions, i.e., the applied load and temperature, preserved the morphology of the specimen.

The shape fixity (R_f) and shape recovery (R_N) ratios are calculated according to Eqs. (1) and (2), respectively.

$$R_f = (\theta_f/\theta_0) \times 100\% \quad (1)$$

$$R_N = (\theta_R/\theta_0) \times 100\% \quad (2)$$

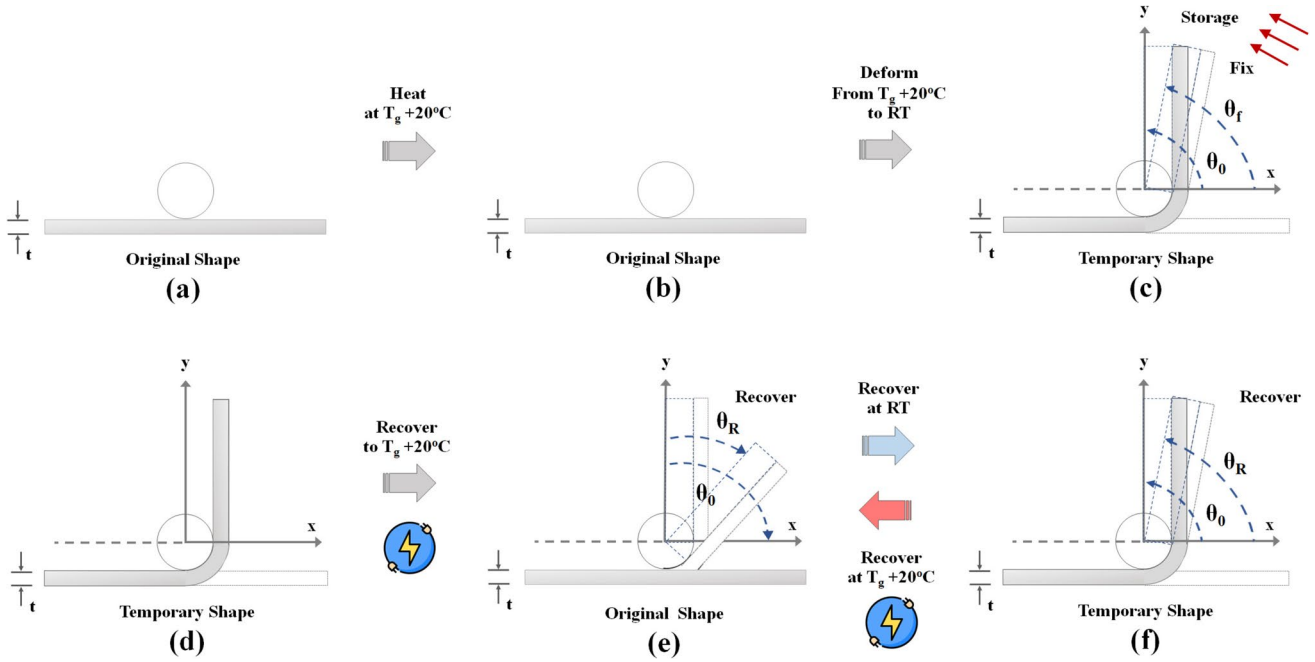

Fig. 1 The setup of 2WSMP programming and recovery process of the specimen

where θ_0 is the intended fixation angle, θ_f is the actual angle after fixation, θ_R is the angle of the specimen after recovery, and N indicates the current shape memory cycle.

Electro-actuated shape memory characterization of the specimen was performed by applying direct current (DC) voltage (DC power supply UNI-T, UDP6720) across the specimen. Experiments were conducted at 8 V for 2 min (the optimal conditions required to achieve sufficiently high temperatures that encompass the recovery temperature range of the composites examined in this study). The temperature changes in the poly(benzoxazine/urethane) composites were monitored using an infrared thermal camera (FLIR C5). The average temperature of each specimen was determined using thermal image processing software (Research IR, FLIR), which made it possible to examine the relationship between the applied voltage and the specimen's temperature.

3 Results and discussion

3.1 Curing behavior of benzoxazine/urethane mixture

Previously, bifunctional bisphenol-A/aniline based benzoxazine (BA-a) polymerized with 2,4-TDI/PPG2000 urethane prepolymer (UP2K) has been demonstrated to possess 2WSMP behavior owing to the phase-separated gradient heterogeneous structure arising from the density differences between the two components (Mora et al. 2023). However, such thermally activated bilayer structure is Limited in the way 2WSMP can be actuated depending on the coefficient of thermal expansion of each individual layer. Therefore, in this work, IPNs based on poly(benzoxazine/urethane) (poly(BA-a:UP2K)) were prepared by sequential curing: first moisture curing of urethane prepolymer followed by thermal curing of benzoxazine to minimize the effect of the gradient heterogeneous structure and allow for the domains to be more evenly dispersed.

First, to verify the complete conversion of isocyanate group with moisture, the mixture of BA-a:UP2K (60:40) was selected as representative to be monitored using FTIR as illustrated in Fig. 2a. The FTIR spectra of the mixture before moisture curing exhibited the unreacted isocyanate characteristic peak of urethane at 2271 cm^{-1} (Parnklang et al. 2019). After moisture curing for 48 h, the results revealed the absence of the unreacted isocyanate characteristic peak at 2271 cm^{-1} along with the appearance of the peaks at 1650 cm^{-1} (urea carbonyl) and 3284 cm^{-1} (urea N–H) corresponding to urea formation. These changes are evident after subjecting the BA-a/UP mixture in a high humidity-controlled environment at RT, signifying that all the remaining isocyanate group reacted with water to form urea linkage (Rimdusit et al. 2011, 2014). Notably, the dibutyltin dilaurate catalyst—commonly employed in conventional urethane synthesis—was deliberately excluded from the methodology presented in this study.

In the next step, the thermal curing behavior of the sequentially cured BA-a:UP2K was monitored using DSC.

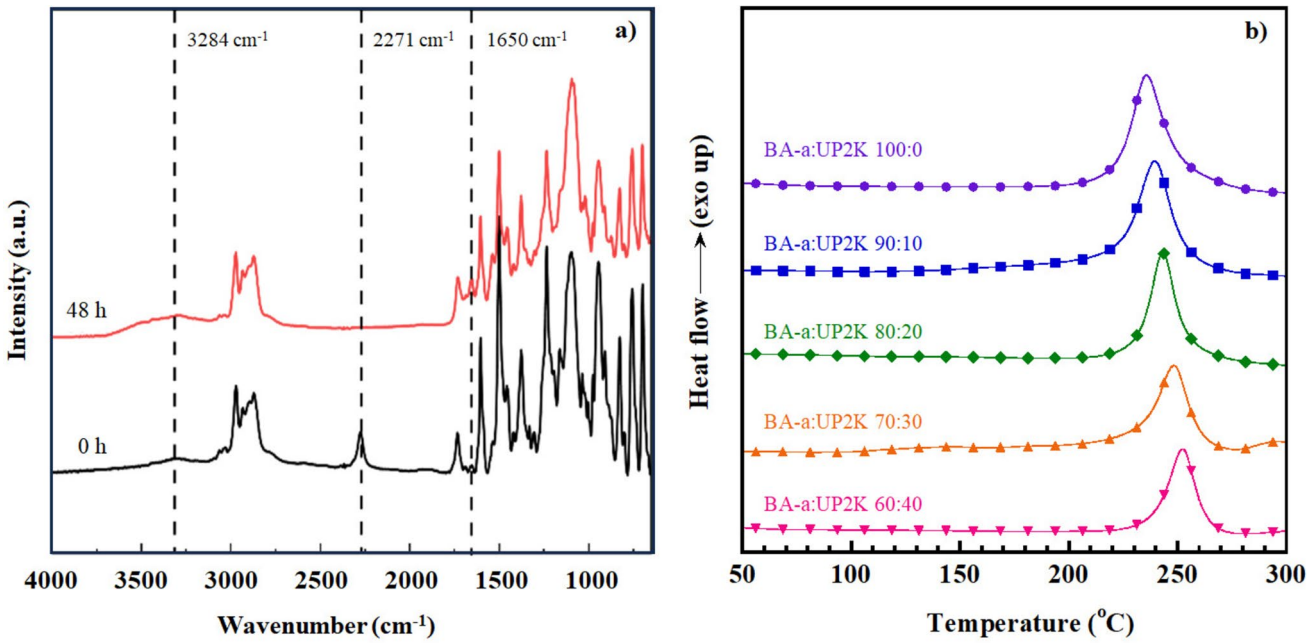

Fig. 2 **a** FTIR spectra comparison of BA-a:UP2K (60:40) before and after moisture curing and **b** DSC thermograms of BA-a:UP2K after moisture curing at various BA-a:UP2K mass ratios

Figure 2b shows the DSC thermograms of the BA-a:UP2K at varying urethane mass ratios from 0 to 40%. As expected by the dilution effect, it was found that the exothermic peak temperature increased as the urethane percentage increased (Rimdusit et al. 2005). The curing peak temperatures were determined to be 235, 239, 243, 248, and 250 °C for BA-a:UP2K ratios of 100:0, 90:10, 80:20, 70:30, and 60:40, respectively. Moreover, the area under the curve was found to decrease due to the lower amount of BA-a available. The presence of exothermic peaks indicated that each mixture specimen was responsive to thermal curing, attributed to the inclusion of BA-a. The values obtained in this work are consistent with previously published sequentially cured BA-a:UP2K utilizing a catalyst (Rimdusit et al. 2014). The results implied that the sequential curing via moisture for urethane followed by thermal curing for BA-a is a potential route to synthesize IPN based on poly(BA-a:UP2K) as proposed in Fig. 3.

3.2 Thermomechanical properties of IPNs based on poly(benzoxazine/urethane)

DMA is a technique typically used to characterize SMP behavior and programming temperature. The E′ values as a function of temperature are illustrated in Fig. 4a. As it can be seen, the E′ value in the glassy state, which is representative of the material stiffness, was found to decrease with increasing PU content from 3.05 GPa of neat poly(BA-a) to 1.07 GPa at 40 wt% PU of poly(BA-a:UP2K), due to the addition of the more flexible polyether chain (Mora et al. 2023). As for the loss tangent curve presented in Fig. 4b, the T_g typically used for the SMP process is derived from the peak temperature of the curve. The existence of two distinct peaks can be detected for all formulations: a first peak at a lower temperature (approximately – 70 °C) and a second at a higher temperature can be assigned to the polyether segment of PU and the polybenzoxazine-dominated domain, respectively. This observed behavior is due to the immiscibility between the polyether segment of PU and the aromatic rings of bifunctional benzoxazine, giving rise to thermodynamically driven phase separation (Rimdusit et al. 2014). Moreover, the peak at a higher temperature is defined as the benchmark for T_g as the urethane segment is already in the rubbery state at RT, while benzoxazine, which serves as the hard segment, is in the glassy state. Experimental findings revealed that increasing the urethane content led to a proportional rise in the intensity of the first peak, whereas the second peak—associated with polybenzoxazine—underwent a thermal shift toward higher temperatures from 176 °C of neat poly(BA-a) to 195, 210, 223, and 245 °C for the BA-a:UP2K ratio of 90:10, 80:20, 70:30, and 60:40 because of the restricted segmental chain movement. The trend in T_g enhancement is similar to the solely thermally cured sample but is lower than the previously reported work because of the different thermal curing procedure (Mora et al. 2023). Nonetheless, the variation in T_g enhancement between thermally and sequentially cured samples remained negligible, Likely

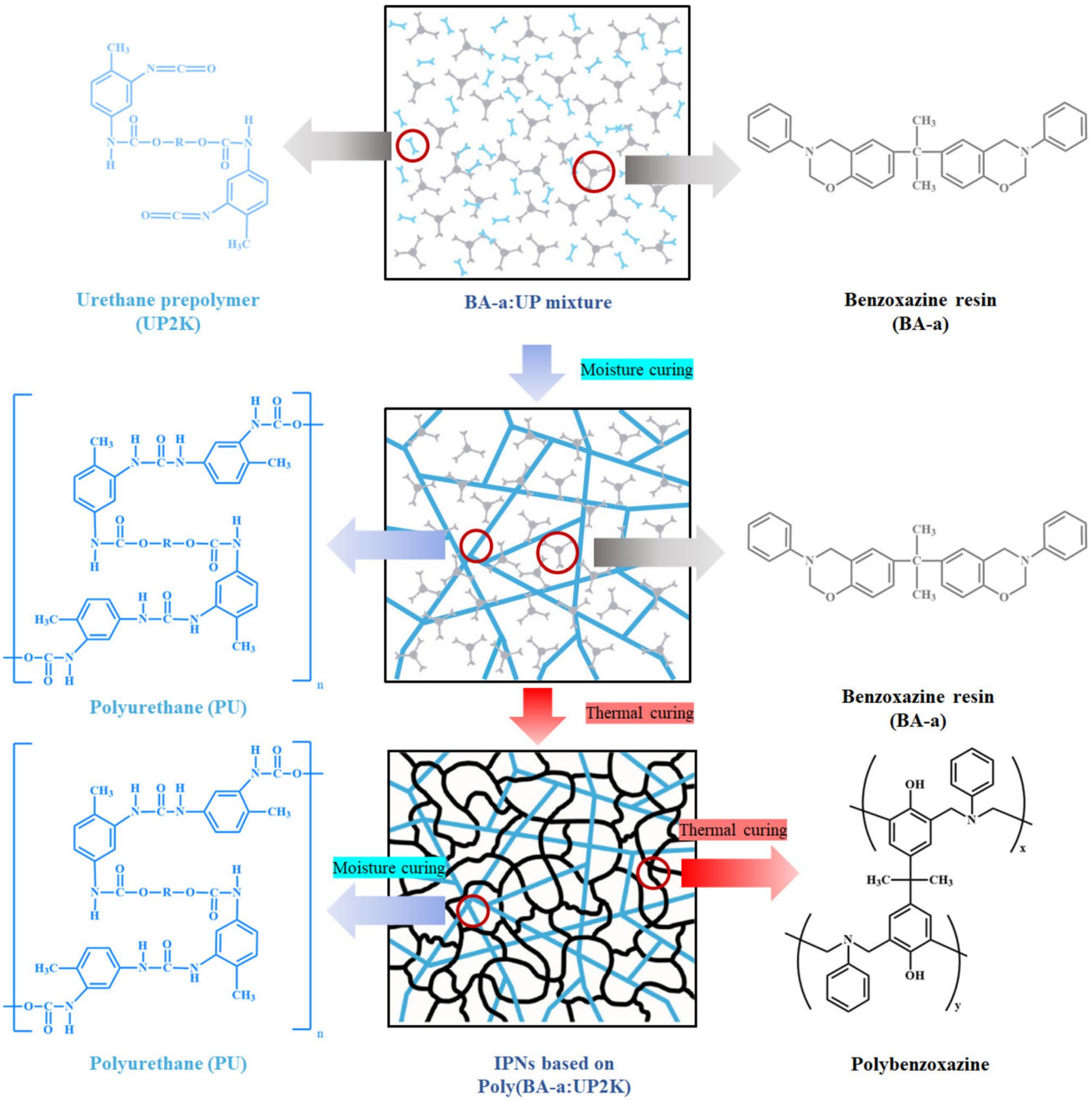

Fig. 3 The sequential curing via moisture curing followed by thermal curing of IPN based on poly(BA-a:UP2K)

due to the Limited availability of isocyanate groups for chemical crosslinking. Consequently, the observed restriction in segmental chain mobility was primarily ascribed to physical entanglement arising from the extended polyether chains. Besides, the amplitude of the second peak reduced drastically at higher urethane content, and some peak towards the lower temperature range emerged in the case of 30 and 40 wt% urethane. This suggests an improvement in damping behavior as well as indicating the increased heterogeneity of the polymer network, which should be conducive to two-way shape memory behavior.

3.3 Morphology observation of IPNs based on poly(benzoxazine/urethane)

The morphology of the sequentially cured poly(BA-a:UP2K) at various BA-a:UP2K mass ratios was investigated by AFM (Fig. 5). The recorded images reveal that phase separation

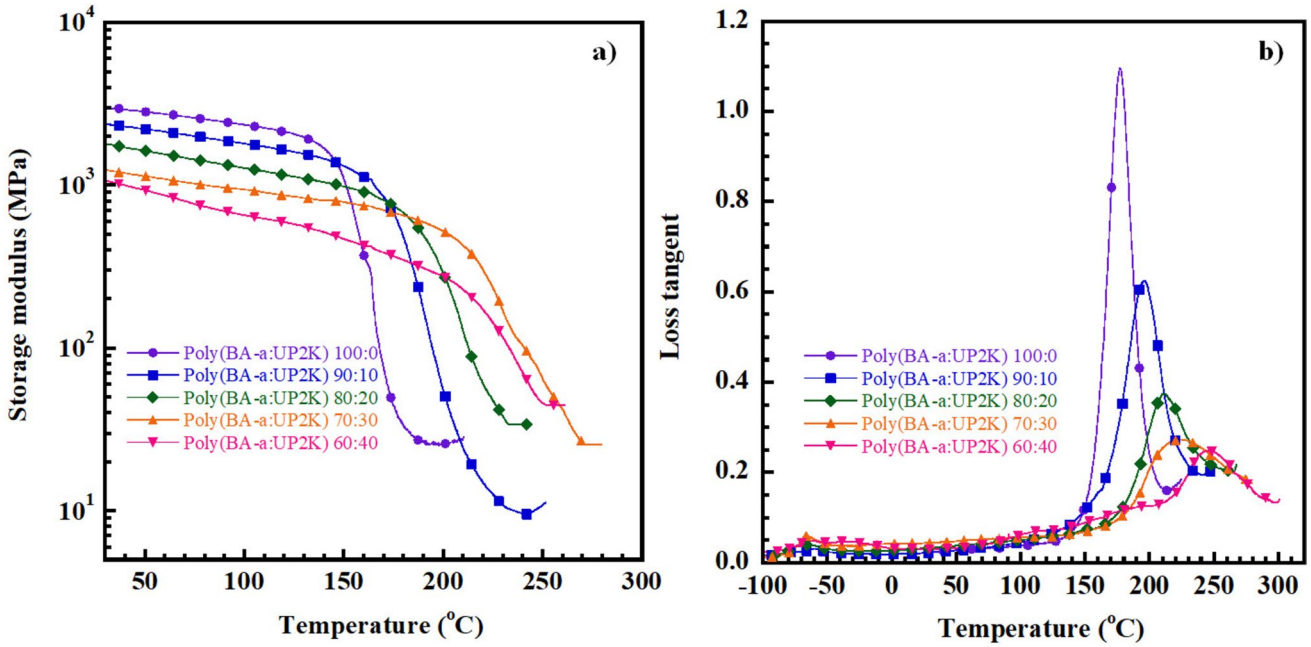

Fig. 4 **a** Storage modulus and **b** loss tangent curves of IPNs based on poly(BA-a:UP2K) at various mass ratios

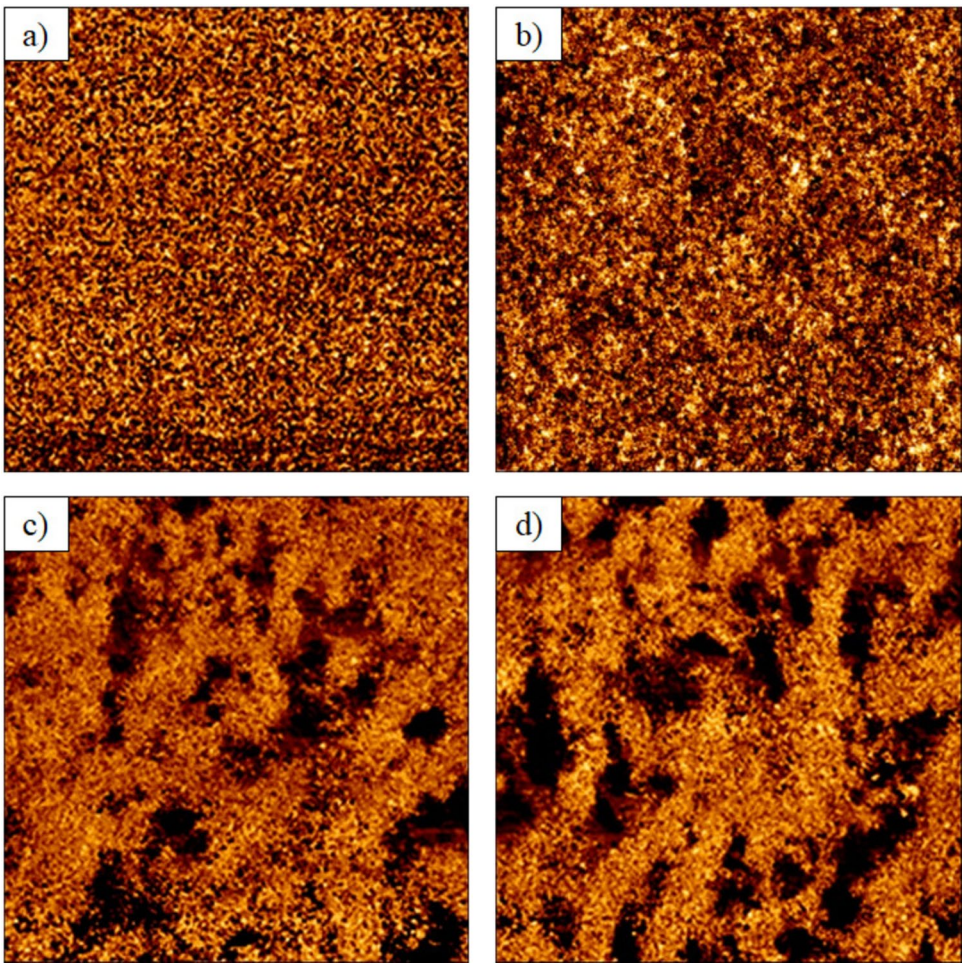

Fig. 5 AFM tapping images of IPNs based on poly(BA-a:UP2K) at various mass ratios: **a** 90:10, **b** 80:20, **c** 70:30, and **d** 60:40. The scan area is 10 μm × 10 μm

occurs between poly(BA-a) phase, which is in yellowish color, and the urethane phase, which is in blackish color. In addition, the domain size of the urethane phase tends to increase with increasing urethane content. The results suggest that the enhancement of the PU content could improve the molecular heterogeneity of IPN, which plays a crucial role in 2WSMP performance.

3.4 Two-way shape memory performance of IPNs based on poly(benzoxazine/urethane)

The fold-deploy method was conducted to demonstrate 2WSMP behavior of sequentially cured poly(BA-a:UP2K) via thermomechanical cycle test as shown in Fig. 6. It is well known that a stationary phase and a reversible phase are necessary for shape fixation and shape recovery, respectively, in order for a polymer system to display SMP properties. For a SMP system to exhibit 2WSMP behavior, either a bilayer structure or a well phase-separated structure is necessary. In this case, the morphology of the sequentially cured IPN should be able to fulfill these two conditions, with BA-a serving as the stationary phase and urethane as the reversible phase, respectively. Initially, the original specimen was heated up to $T_g + 20$ °C to ensure that the benzoxazine-rich domain was in the rubbery state before it was subjected to deformation (step (a)). Afterwards, the sample was cooled down to RT under constant applied stress, increasing the deformation angle to fix the temporary shape (step (b)). After removing load, the sample was restored to its original shape under heating up to $T_g + 20$ °C (step (c)). In this step, the specimen shrank as a result of the stress in the SMP based on the IPN network being released as a driving force (switch opens) and the elastomer PU phase being stored with potential energy and macroscopically compressed (push spring). Then, the sample was automatically recovered into its temporary shape after re-cooling to RT without reprogramming (step (d)). In this step, the specimen experienced cooling-induced expansion as a result of the potential energy being released by the elastic recovery effect of the PU phase and the IPN being remembered and fixed in its temporary shape (Mora et al. 2023).

This enables external stress-free shape reversion between the two shapes by cycling between $T_g + 20$ °C and RT. Figure 7a, b displays the effect of PU content on the R_f and R_N of the original and temporary shapes, which are calculated from Eqs. (1) and (2), respectively. The R_f values at the original shapes of IPN decreased from $97 \pm 3\%$ to $92 \pm 2\%$, while those at the temporary shapes also decreased from $96 \pm 2\%$

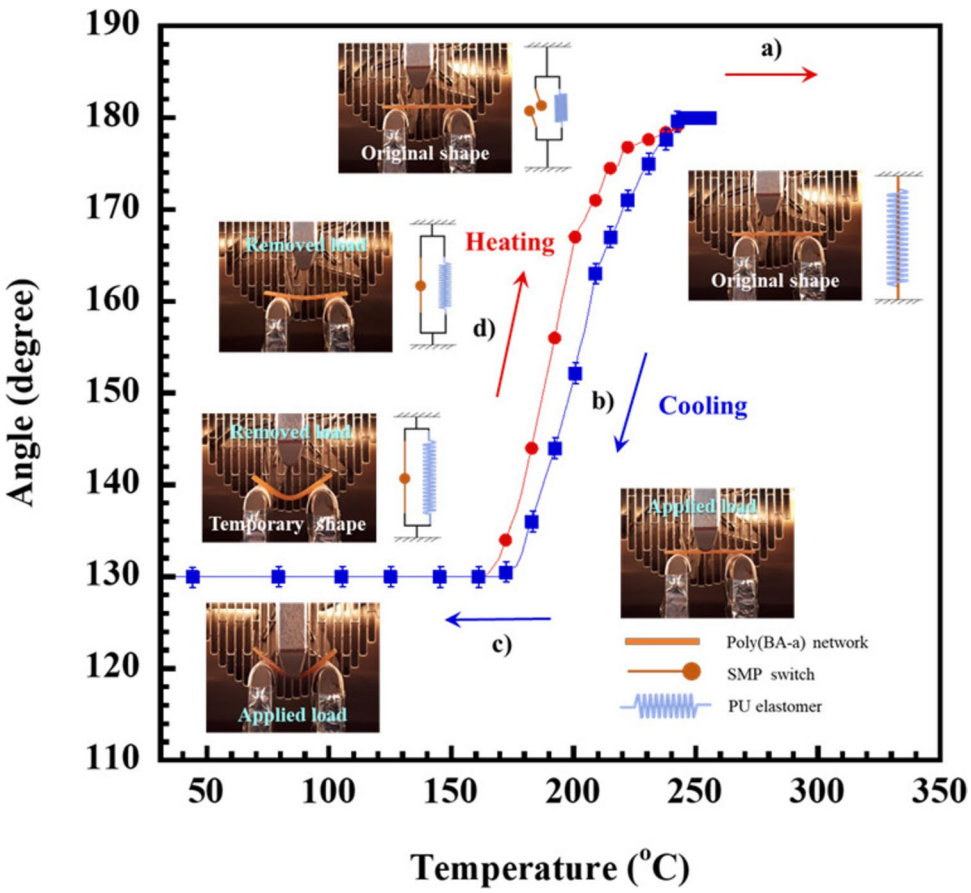

Fig. 6 Two-way shape memory programming of IPNs based on poly(BA-a:UP2K)

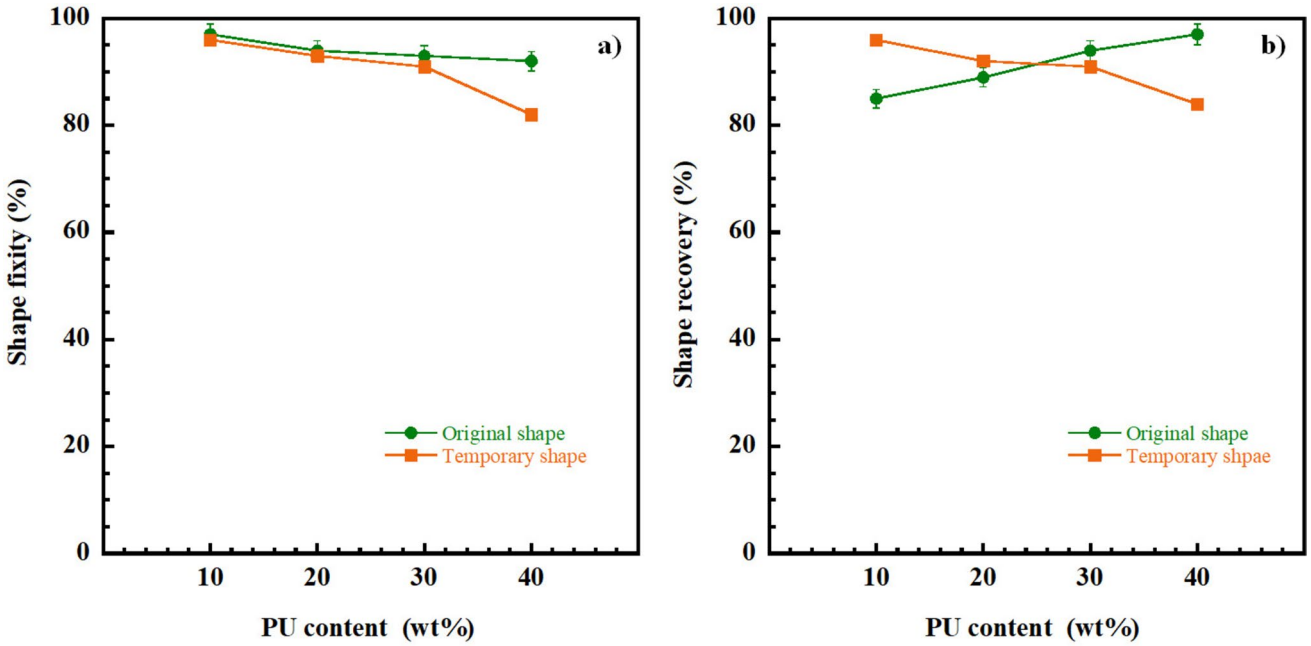

Fig. 7 **a** Shape fixity and **b** shape recovery of the original and temporary shapes of IPNs at different PU contents

to 82 ± 2%. It was found that as the PU content increased, the R_f values at the original and temporary shapes of IPN decreased due to the higher reversible PU phase acting as a spring segment (Wu et al. 2014a). With an increase in PU content, the R_N values of IPN to the original shape increased from 85 ± 2% to 97 ± 3%, thanks to the higher chain flexibility of PU leading to high shape recovery under heating (Prathumrat et al. 2017a). Furthermore, the R_N values of the IPN to the temporary shape decreased from 96 ± 3% to 84 ± 2% with the presence of PU because the restricted PU phase in the IPN network led to low shape recovery while cooling (Ke et al. 2020; Posada-Murcia et al. 2022). Overall, sequential curing yielded marginally enhanced R_f and R_N performance metrics relative to those achieved through conventional thermal curing methods (Mora et al. 2023). This may be attributed to the limited increase in crosslinking density following PU incorporation; as a result, the matrix experiences comparatively less constraint during post-cooling expansion.

3.5 Thermomechanical properties of CFF-reinforced poly(benzoxazine/urethane) composites

Nevertheless, despite the improved shape memory performance by sequential curing, the stiffness of the specimen is relatively high, limiting its flexibility and possible deformation angle. Accordingly, the incorporation of CFF into the IPN matrix was intended to enhance the shape memory properties and utility. Poly(BA-a:UP2K) at 70:30 was selected as a representative formulation to be reinforced with CFF due to its generally good shape memory performance and thermomechanical properties. Figure 8 illustrates the storage modulus of poly(BA-a:UP2K) at 70:30 with a loading of 3–7 wt% CFF. IPNs containing CFF at concentrations of 0, 3, 5, and 7 wt% enhanced their storage modulus to 1.24, 1.35, 1.53, and 1.71 GPa in a glassy state at 30 °C, respectively. This occurred due to the rigidity introduced by the stiff CFF, which enhanced the modulus of the specimen and improved its shape fixity (Soto et al. 2018).

According to the loss tangent curve, the T_g values of IPNs incorporating CFF at 0, 3, 5, and 7 wt% were increased to 223, 230, 234, and 238 °C, respectively. This could be due to the higher CFF concentration restricting polymer chain segmental mobility. The results implied that the reinforcement of CFF into the IPNs not only improved the stiffness of the composites but also enhanced service temperature by increasing T_g of the composites, which is desirable in high-performance applications, such as aerospace or automotive.

3.6 Electrothermal actuation effect of CFF-reinforced poly(benzoxazine/urethane) composites

To study the electro-induced shape memory effect of the CFF-reinforced IPN based on poly(BA-a:UP2K) actuated by electric current, the electrothermal actuation of the composite at various CFF contents was investigated. The generated temperature as a function of time of the composite specimen actuated by electric voltage (8 V) is shown in Fig. 9. It is evident that increasing the time of exposure enhances

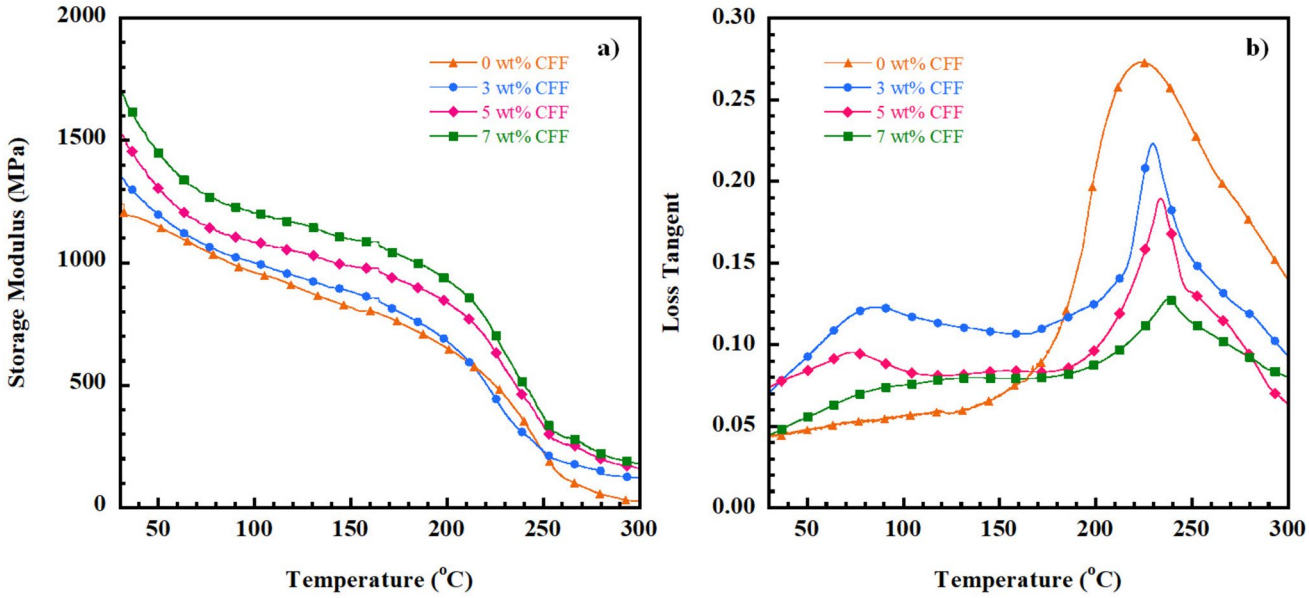

Fig. 8 **a** Storage modulus and **b** loss tangent curves of poly(BA-a:UP2K) composites at various CFF contents

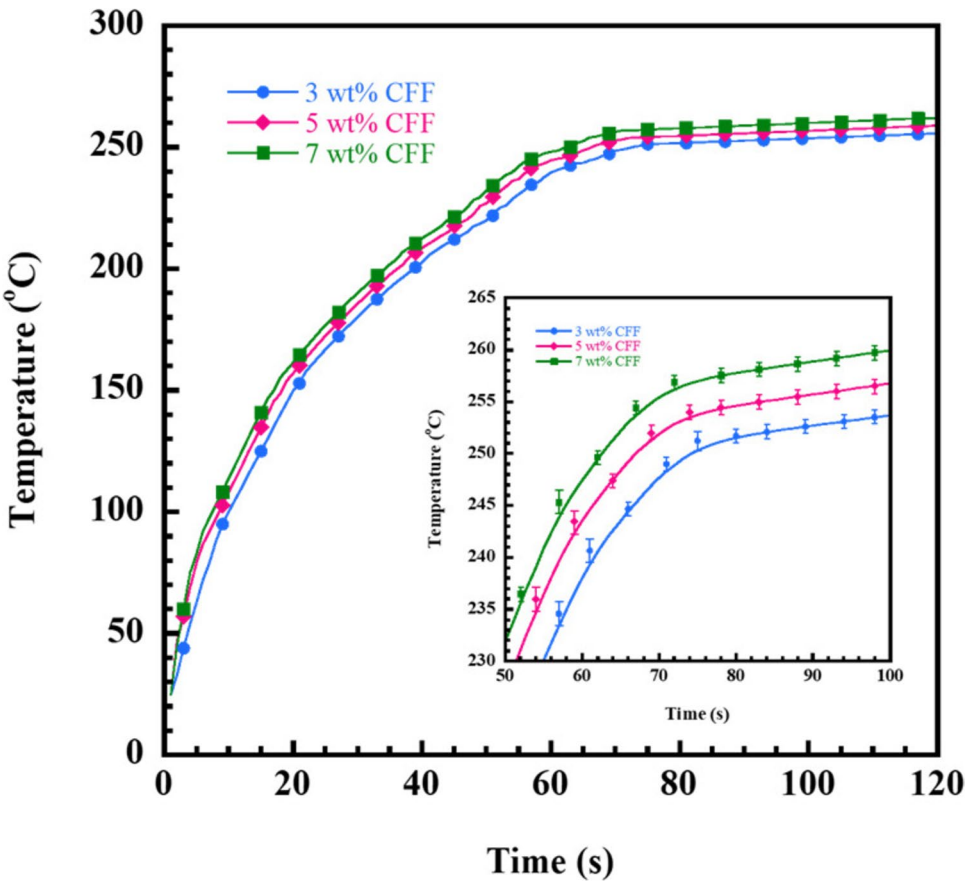

Fig. 9 The generated temperature of poly(BA-a:UP2K) composites at various CFF contents under actuation of electric current

the heat flux density of the sample and its temperature. In addition, the generated temperature of the poly(BA-a:UP2K) composite at CFF of 3, 5, and 7 wt% could reach equilibrium at 256 ± 1 °C, 259 ± 1 °C, and 262 ± 1 °C within 82 ± 2 s, 89 ± 1 s, and 108 ± 2 s, respectively. The results suggested that the presence of CFF in the composites could generate

indirect Joule heating by electric current due to the electrothermal actuation effect of CFF. Therefore, 8 V was used to trigger the specimen for further 2WSMP investigations under the electro actuation of the specimen.

3.7 Electro-induced two-way shape memory effect of CFF-reinforced poly(benzoxazine/urethane) composites

The electro-induced two-way shape memory effect of the CFF-reinforced IPN based on poly(BA-a:UP2K) at various CFF contents actuated by electric voltage (8 V) was investigated. After thermal programming into the composite specimen, the shape recovery to original shape (Fig. 10a) and temporary shape (Fig. 10b) as a function of electro actuated time was systematically determined. The SMP performance of the CFF-reinforced IPN composites is reported in Table 1. The results from Fig. 10 showed that all IPN composites could recover their shape into original shape (intended fixation angle of ~180°) when actuated by electric current until reaching their ~T_g + 20 °C and meet their maximum shape recovery values. When heat from electrothermal actuation was removed, all IPN composites were automatically recovered to their temporary shape (intended fixation angle of ~130°) until cooled down to RT. The results suggested that the developed CFF-reinforced IPN based on poly(BA-a:UP2K) exhibited 2WSME actuated by electric current.

Moreover, from Table 1, the results showed that the shape fixity values of the original and temporary shapes were increased with increasing CFF content compared with the IPN sample without CFF (93 ± 2% for R_f at original shape and 91 ± 1% for R_f at temporary shape), due to the rigid nature of CFF restricting the chain mobility of polymer in the system (Likitaporn et al. 2017). The R_N of both original and temporary shapes of the composites improved from 94 ± 2% and 91 ± 2% of neat IPN, respectively, with increasing CFF content up to 3 wt%. This is attributed to the CFF capacity to form a thermally conductive network, which accelerated heat transfer inside the IPN matrix. Additionally, the R_N values of the composites at CFF content beyond

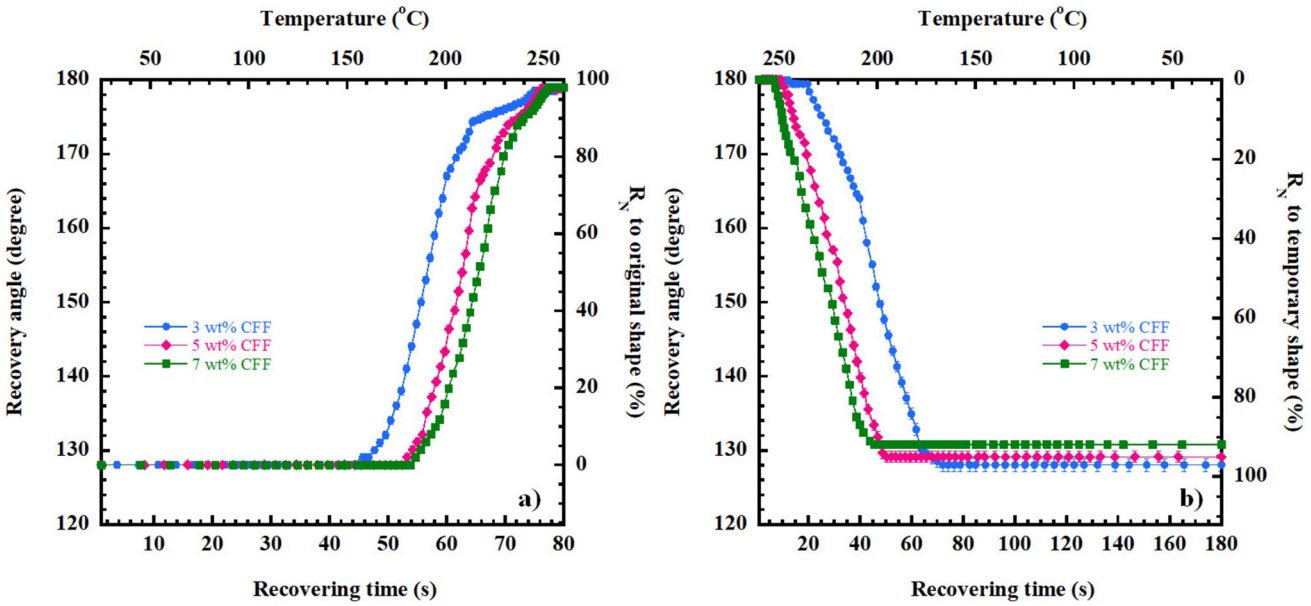

Fig. 10 Shape recovery to **a** original shape and **b** temporary shape as a function of electro actuated time, recovery angle, and temperature of poly(BA-a:UP2K) composites at various CFF contents

Table 1 Two-way shape memory performance of poly(BA-a:UP2K) composites at various CFF contents

Property	CFF content					
	Original shape			Temporary shape		
	3%	5%	7%	3%	5%	7%
Shape fixity, R_f (%)	97 ± 2	98 ± 2	98 ± 2	97 ± 2	97 ± 2	98 ± 2
Shape recovery, R_N (%)	97 ± 2	98 ± 1	98 ± 1	97 ± 1	95 ± 2	92 ± 2
Recovering time (s)	76 ± 1	75 ± 1	74 ± 1	66 ± 1	44 ± 2	43 ± 1

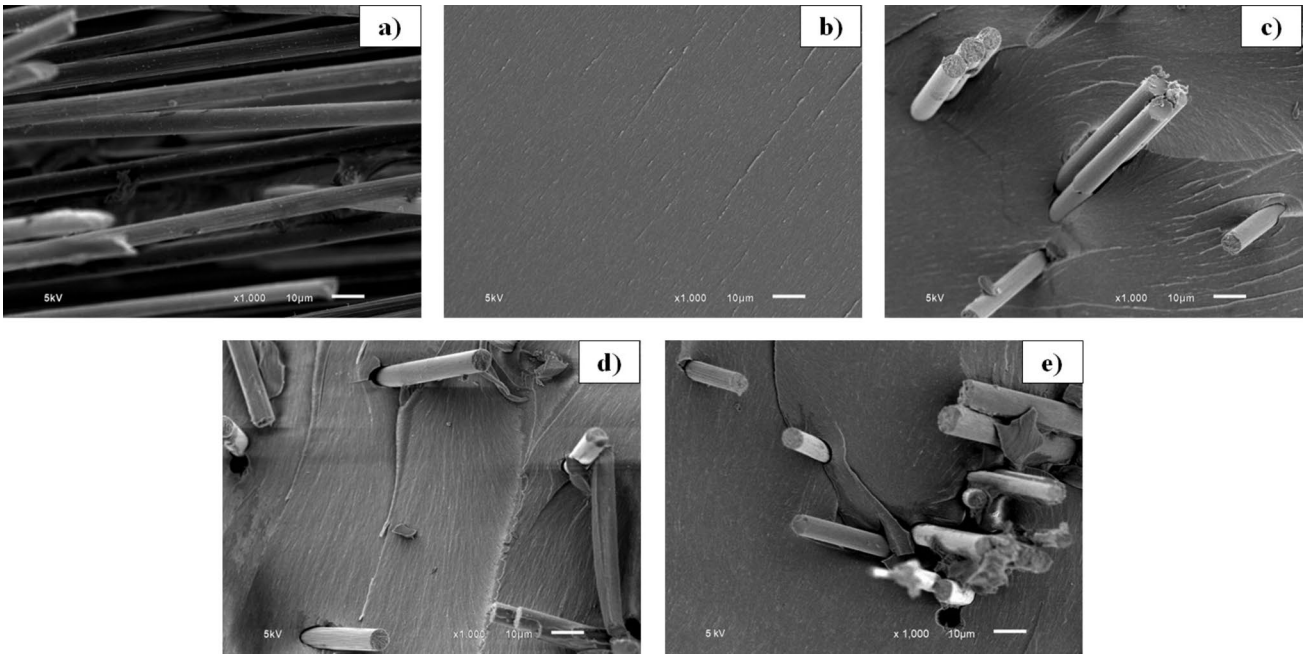

Fig. 11 SEM images of **a** neat CFF, cross section **b** poly(BA-a:UP2K) at 70/30 wt% and poly(BA-a:UP2K) composite at **c** 3 wt%, **d** 5 wt%, and **e** 7 wt% of CFF

3 wt% were slightly decreased with the addition of CFF. This may stem from the rigidity of the CFF, which Likely impedes the mobility of the IPN chains during shape transition between the permanent and temporary states. Furthermore, faster recovering time of the composites was obtained with increasing CFF content. This might be due to the electrothermal actuation effect of CFF which enhances the generated temperature onto the specimen and consequently promotes recovering ability faster. The results indicated that incorporation of such filler by at least 3 wt% improved the shape memory performance as the strain energy of the IPN-reinforced CFF is higher than that of neat IPN.

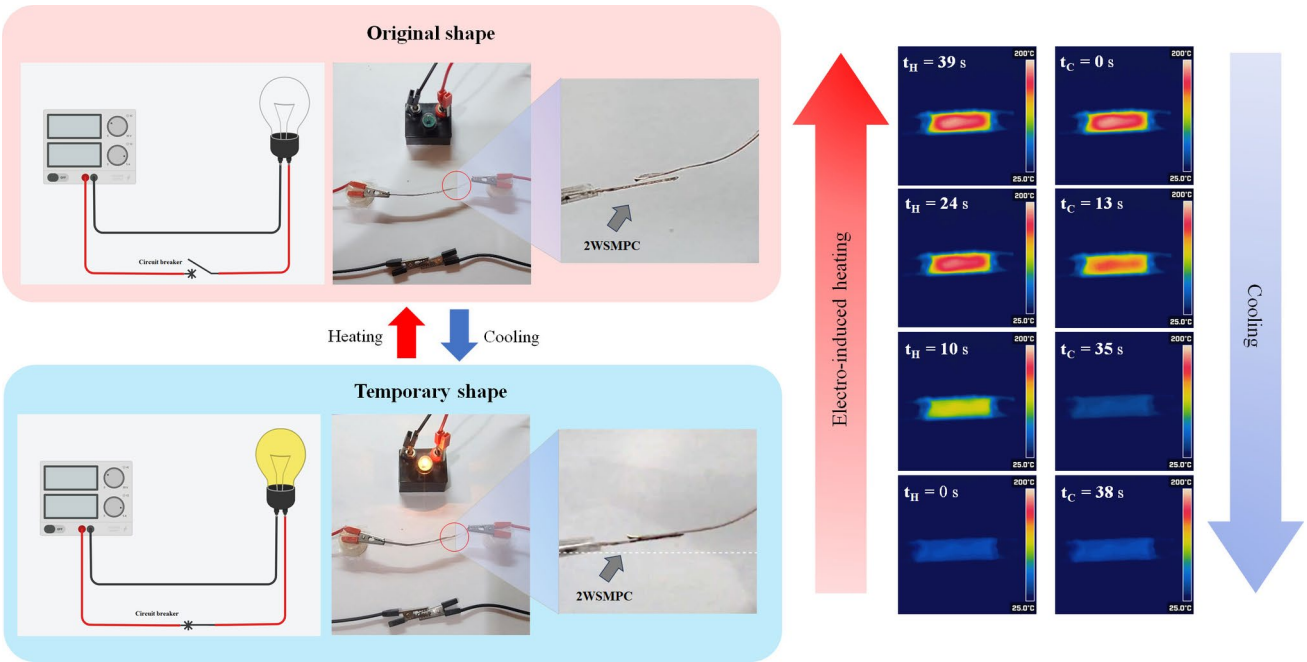

Fig. 12 Electric circuit breaker of the two-way shape memory polymer composite based on 3 wt% CFF-reinforced poly(BA-a:UP2K) composites

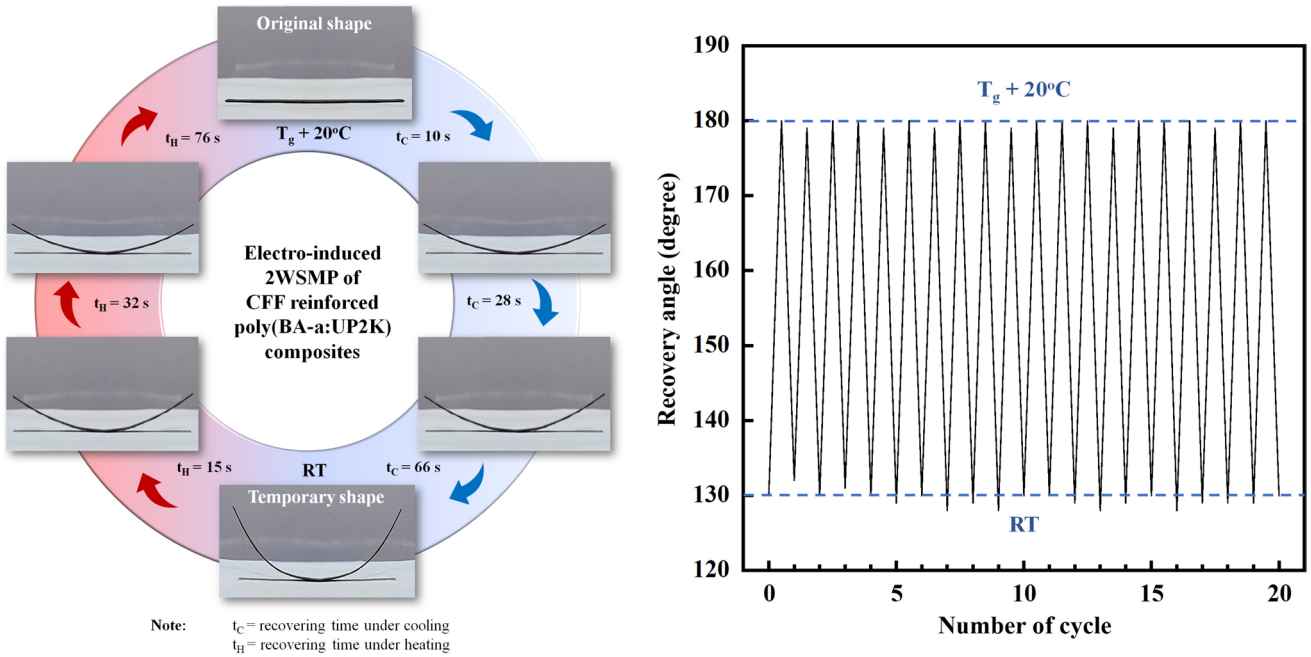

Fig. 13 Repeated fold-deploy cycles of electro-induced 2WSMP of 3 wt% CFF-reinforced IPN based on poly(BA-a:UP2K) actuated by electric current

3.8 Morphology of CFF-reinforced poly(benzoxazine/urethane) composites

The morphology of poly(benzoxazine/urethane) composite filled with CFF was observed by SEM. The morphology of neat CFF and cross-sectional micrographs of IPN composites at various amounts of CFF are presented in Fig. 11. The neat CFF with a random arrangement and a fiber diameter of approximately 7 µm is shown in Fig. 11a. The surface of pure IPN based on poly(BA-a:UP2K) is rather smooth, as seen in Fig. 11b. Images from composites containing 3 and 5 wt% of CFF are shown in Fig. 11b, c, which demonstrate that the CFF is distributed in the matrix and exhibits good adhesion between the CFF and the IPN matrix. Conversely, Fig. 11e demonstrates that agglomeration at 7 wt% was caused by an excessive amount of filler. This could be the cause of the decreased shape recovery of the previous results.

3.9 Feasibility of two-way shape memory polymer composite based on CFF-reinforced poly(benzoxazine/urethane) in electric circuit breaker application

In this research, an intelligent electro-controlled electric circuit breaker utilizing a 2WSMPC based on 3 wt% CFF-reinforced IPN based on poly(BA-a:UP2K) was examined. Figure 12 illustrates the electric circuit functioning with the implementation of electro-induced 2WSMPC as the breaker bridge materials. The temperature versus electro actuated time of the specimen was also recorded by a thermal camera. The 2WSMPC acted as a switching mechanism to control light bulb functionality by alternating between its original and temporary shapes in response to an applied voltage (8 V). In the 2WSMPC programming, the sample of 3 wt% CFF-reinforced IPN was subjected to heating at around T_g + 20 °C without any load. The sample was subsequently cooled to RT while being shaped into a temporary form, after which the applied force was released to yield the programmed 2WSMPC specimen. In the recovery step, the programmed 2WSMPC based on CFF-reinforced poly(BA-a:UP2K) in the temporary shape was installed in the circuit loop. When the circuit was closed, the flow of electric current resulted in turning on the Light. Upon electrical activation and heating to elevated temperatures, the sample autonomously reverted from its temporary configuration to its original shape, thereby interrupting the circuit by opening loops and switching off the Light. Following circuit disconnection and subsequent cooling, the sample transitioned from its original configuration back to its temporary shape, thereby completing the circuit and reactivating the light source. The results revealed that 3 wt% CFF-reinforced IPN based on poly(BA-a:UP2K) showed electro-induced 2WSME actuated by electric current, which is suitable for the electric circuit breaker application.

The electro-induced two-way shape memory performance of the 3 wt% CFF-reinforced IPN based on poly(BA-a:UP2K)

activated by electric current was also examined by repeated fold-deploy cycles, as illustrated in Fig. 13. According to the results, the recovery angle values between original and temporary shapes of the poly(BA-a:UP2K) composites were insignificant up to 20 cycles, suggesting that two-way shape memory performance of the specimen was extremely stable.

4 Conclusions

In summary, in this work, the electro-induced two-way shape memory effect was demonstrated in novel interpenetrating polymer networks (IPNs) based on poly(benzoxazine/urethane) reinforced with carbon fiber felt (CFF). IPNs of benzoxazine and urethane were fabricated by sequential curing; moisture curing first followed by thermal curing. Increasing the mass ratio of urethane resulted in the improvement of two-way shape memory performance in terms of both shape fixity (original shape: 92–98%, temporary shape: 82–95%) and shape recovery ratios (original shape: 85–97%, temporary shape: 84–95%) when compared to its conventional thermally cured counterpart. The results suggested that the addition of PU at 30 wt% exhibited good thermomechanical properties and relatively high two-way shape memory performance. In terms of electro-induced 2WSMP performance, the shape fixity for both original and temporary shape of IPN composites was in the range of 97–98% with the reinforcement of CFF. Additionally, the results revealed that shape recovery to original shape at $T_g + 20$ °C via electric current trigger of the composites was 97–98%, while those to temporary shape at RT were 92–97%. Moreover, the incorporation of CFF up to 3 wt% resulted in further enhancement in the two-way shape memory performance which was reversely recovered between original and temporary shapes at least 20 cycles, illustrating the potential of such SMP composites in advanced electric circuit breaker applications.

Author contribution The data curation and methodology were performed by Kittipon Bunyanuwat. The original draft was written by Kittipon Bunyanuwat and Panuwat Luengrojanakul. The visualization of the results was performed by Phattarin Mora and Panuwat Luengrojanakul. Formal analysis was performed by Chaweewan Sapcharoenkun and Jinying Yuan. The formal manuscript was reviewed and edited by Phattarin Mora and Panagiotis Karagiannidis. Funding acquisition and supervision were performed by Sarawut Rimdusit.

Funding The authors would like to express their sincere appreciation for the financial support to the Second Century Fund (C2F), Chulalongkorn University, 90th Anniversary of Chulalongkorn University Fund (Ratchadapiseksomphot Endowment Fund), National Research Council of Thailand (NRCT) and Chulalongkorn University (N42A660910), and Thailand Science Research and Innovation Fund Chulalongkorn University (BCG_FF_68_206_2100_030).

Data availability The authors confirm that all underlying data of this work are available within the article itself.

Declarations

Competing interests The authors have no relevant financial or non-financial interests to disclose.

Conflicts of Interest The authors declare no conflict of interest.

References

Amornkitbamrung L, Srisaard S, Jubsilp C, Bielawski CW, Um SH, Rimdusit S (2020) Near-infrared light responsive shape memory polymers from bio-based benzoxazine/epoxy copolymers produced without using photothermal filler. Polymer 209:122986. https://doi.org/10.1016/j.polymer.2020.122986

Amornkitbamrung L, Leungpuangkaew S, Panklang T, Jubsilp C, Ekgasit S, Um SH, Rimdusit S (2022) Effects of glutaric anhydride functionalization on filler-free benzoxazine/epoxy copolymers with shape memory and self-healing properties under near-infrared light actuation. J Sci-Adv Mater Dev 7(3):100446. https://doi.org/10.1016/j.jsamd.2022.100446

Arun DI, Santhosh Kumar KS, Satheesh Kumar B, Chakravarthy P, Dona M, Santhosh B (2019) High glass-transition polyurethane-carbon black electro-active shape memory nanocomposite for aerospace systems. Mater Sci Technol 35(5):596–605. https://doi.org/10.1080/02670836.2019.1575054

Chen S, Yang S, Li Z, Xu S, Yuan H, Chen S, Ge Z (2015) Electroactive two-way shape memory polymer laminates. Polym Compos 36(3):439–444. https://doi.org/10.1002/pc.22958

Gong X, Liu L, Liu Y, Leng J (2016) An electrical-heating and self-sensing shape memory polymer composite incorporated with carbon fiber felt. Smart Mater Struct 25(3):035036. https://doi.org/10.1088/0964-1726/25/3/035036

Goyal A, Ur Rahman H, Ghani SAC (2021) Experimental investigation & optimisation of wire electrical discharge machining process parameters for Ni49Ti51 shape memory alloy. J King Saud Univ Eng Sci 33(2):129–135. https://doi.org/10.1016/j.jksues.2020.01.003

Gu S, Jana S (2014) Effects of polybenzoxazine on shape memory properties of polyurethanes with amorphous and crystalline soft segments. Polymers (Basel) 6:1008–1025. https://doi.org/10.3390/polym6041008

Huang X, Panahi-Sarmad M, Dong K, Li R, Chen T, Xiao X (2021) Tracing evolutions in electro-activated shape memory polymer composites with 4D printing strategies: a systematic review. Compos Part A Appl Sci Manuf 147:106444. https://doi.org/10.1016/j.compositesa.2021.106444

Ishida H, Allen JD (1996) Physical and mechanical characterization of near-zero shrinkage polybenzoxazines. J Polym Sci Pol Phys 34(6):1019–1030. https://doi.org/10.1002/(SICI)

1099-0488(19960430)34:6%3c1019::AID-POLB1%3e3.0.CO;2-T
Ishida H, Agag T (2011) Handbook of benzoxazine resins. Elsevier, Amsterdam, The Netherlands
Ishida H (1996) Process for preparation of benzoxazine compounds in solventless systems. US Patent 5,543,516 A
Jamnongpak W, Tiptipakorn S, Arumugam H, Charoensuk K, Karagiannidis P, Rimdusit S (2024) Development of NIR light-responsive shape memory composites based on bio-benzoxazine/bio-urethane copolymers reinforced with graphene. Nanoscale Adv 6(2):499–510. https://doi.org/10.1039/D3NA00647F
Ke D, Chen Z, Momo ZY, Jiani W, Xuan C, Xiaojie Y, Xueliang X (2020) Recent advances of two-way shape memory polymers and four-dimensional printing under stress-free conditions. Smart Mater Struct 29(2):023001. https://doi.org/10.1088/1361-665x/ab5e6d
Lee AY, An J, Chua CK (2017) Two-way 4D printing: a review on the reversibility of 3D-printed shape memory materials. Engineering 3(5):663–674. https://doi.org/10.1016/J.ENG.2017.05.014
Leng J, Lv H, Liu Y, Du S (2007) Electroactivate shape-memory polymer filled with nanocarbon particles and short carbon fibers. Appl Phys Lett 91(14):144105. https://doi.org/10.1063/1.2790497
Leng J, Lan X, Liu Y, Du S (2011) Shape-memory polymers and their composites: stimulus methods and applications. Prog Mater Sci 56(7):1077–1135. https://doi.org/10.1016/j.pmatsci.2011.03.001
Leungpuangkaew S, Amornkitbamrung L, Phetnoi N, Sapcharoenkun C, Jubsilp C, Ekgasit S, Rimdusit S (2023) Magnetic- and light-responsive shape memory polymer nanocomposites from bio-based benzoxazine resin and iron oxide nanoparticles. Adv Ind Eng Polym Res 6(3):215–225. https://doi.org/10.1016/j.aiepr.2023.01.003
Li J, Rodgers WR, Xie T (2011) Semi-crystalline two-way shape memory elastomer. Polymer 52(23):5320–5325. https://doi.org/10.1016/j.polymer.2011.09.030
Li M, Chen J, Shi M, Zhang H, Ma PX, Guo B (2019) Electroactive antioxidant polyurethane elastomers with shape memory property as non-adherent wound dressing to enhance wound healing. Chem Eng J 375:121999. https://doi.org/10.1016/j.cej.2019.121999
Likitaporn C, Mora P, Tiptipakorn S, Rimdusit S (2017) Recovery stress enhancement in shape memory composites from silicon carbide whisker–filled benzoxazine-epoxy polymer alloy. J Intell Mater Syst Struct 29(3):388–396. https://doi.org/10.1177/1045389X17708041
Maksimkin AV, Dayyoub T, Telyshev DV, Gerasimenko AY (2022) Electroactive polymer-based composites for artificial muscle-like actuators: a review. Nanomaterials. https://doi.org/10.3390/nano12132272
Mora P, Jubsilp C, Ahn C-H, Rimdusit S (2023) Two-way thermo-responsive thermoset shape memory polymer based on benzoxazine/urethane alloys using as self-folding structures. Adv Ind Eng Polym Res 6(1):13–23. https://doi.org/10.1016/j.aiepr.2022.09.001
Ohm C, Brehmer M, Zentel R (2010) Liquid crystalline elastomers as actuators and sensors. Adv Mater 22(31):3366–3387. https://doi.org/10.1002/adma.200904059
Parnklang T, Boonyanuwat K, Mora P, Ekgasit S, Rimdusit S (2019) Form-stable benzoxazine-urethane alloys for thermally reversible light scattering materials. Express Polym Lett 13:65–83. https://doi.org/10.3144/expresspolymlett.2019.7
Phetnoi N, Amornkitbamrung L, Charoensuk K, Sapcharoenkun C, Jubsilp C, Ekgasit S, Rimdusit S (2024) Fast magnetic-responsive shape memory composites from bio-based benzoxazine/polyglycerol polyglycidyl ether copolymers highly filled with iron oxide nanoparticles. Compos Part A Appl Sci Manuf 186:108398. https://doi.org/10.1016/j.compositesa.2024.108398
Posada-Murcia A, Uribe-Gomez JM, Förster S, Sommer J-U, Dulle M, Ionov L (2022) Mechanism of behavior of two-way shape memory polymer under constant strain conditions. Macromolecules 55(5):1680–1689. https://doi.org/10.1021/acs.macromol.1c02564
Prathumrat P, Tiptipakorn S, Rimdusit S (2017b) Multiple-shape memory polymers from benzoxazine-urethane copolymers. Smart Mater Struct. https://doi.org/10.1088/1361-665X/aa6d47
Prathumrat P, Tiptipakorn S, Rimdusit S (2017a) Multiple-shape memory polymers from benzoxazine-urethane copolymers. Smart Mater Struct 26(6). https://doi.org/10.1088/1361-665X/aa6d47
Pringpromsuk S, Xia H, Ni Q-Q (2020) Multifunctional stimuli-responsive shape memory polyurethane gels for soft actuators. Sens Actuator A Phys 313:112207. https://doi.org/10.1016/j.sna.2020.112207
Qi X, Dong P, Liu Z, Liu T, Fu Q (2016) Selective localization of multi-walled carbon nanotubes in bi-component biodegradable polyester blend for rapid electroactive shape memory performance. Compos Sci Technol 125:38–46. https://doi.org/10.1016/j.compscitech.2016.01.023
Ratna D, Karger-Kocsis J (2011) Shape memory polymer system of semi-interpenetrating network structure composed of crosslinked poly (methyl methacrylate) and poly (ethylene oxide). Polymer 52(4):1063–1070. https://doi.org/10.1016/j.polymer.2010.12.054
Rimdusit S, Pirstpindvong S, Tanthapanichakoon W, Damrongsakkul S (2005) Toughening of polybenzoxazine by alloying with urethane prepolymer and flexible epoxy: a comparative study. Polym Eng Sci 45(3):288–296. https://doi.org/10.1002/pen.20273
Rimdusit S, Bangsen W, Kasemsiri P (2011) Chemorheology and thermomechanical characteristics of benzoxazine-urethane copolymers. J Appl Polym Sci. https://doi.org/10.1002/app.34170
Rimdusit S, Sudjidjune M, Jubsilp C, Tiptipakorn S (2014) Enhanced film forming ability of benzoxazine- urethane hybrid polymer network by sequential cure method. J Appl Polym Sci. https://doi.org/10.1002/app.40502
Rimdusit S, Jubsilp C, Tiptipakorn S (2013) Alloys and composites of polybenzoxazines: properties and applications. Springer, New York
Rouf S, Raina A, Irfan Ul Haq M, Naveed N, Jeganmohan S, Farzana Kichloo A (2022) 3D printed parts and mechanical properties: influencing parameters, sustainability aspects, global market scenario, challenges and applications. Adv Ind Eng Polym Res 5(3):143–158. https://doi.org/10.1016/j.aiepr.2022.02.001
Ruenpanya K, Mora P, Karagiannidis P, Bunyanuwat K, Rimdusit S (2024) Magnetic-responsive triple shape memory polymer from bio-based benzoxazine/urethane polymer alloys with iron oxide nanoparticles. Adv Ind Eng Polym Res. https://doi.org/10.1016/j.aiepr.2024.07.001
Sánchez CP, Jérôme C, Noels L, Vanderbemden P (2022) Review of thermoresponsive electroactive and magnetoactive shape memory polymer nanocomposites. ACS Omega 7(45):40701–40723. https://doi.org/10.1021/acsomega.2c05930
Schäfer H, Hartwig A, Koschek K (2018) The nature of bonding matters: benzoxazine based shape memory polymers. Polymer 135:285–294. https://doi.org/10.1016/j.polymer.2017.12.029
Schäfer H, Kolberg A, Gockeln M, Kun R, Balzer BN, Koschek K (2019) Influence of free PCL in PCL/PBA-a copolymers and blends on morphology, thermo-mechanical and shape memory properties. Polym Test 77:105888. https://doi.org/10.1016/j.polymertesting.2019.05.004
Shao L-n, Dai J, Zhang Z-x, Yang J-h, Zhang N, Huang T, Wang Y (2015) Thermal and electroactive shape memory behaviors of poly(l-lactide)/thermoplastic polyurethane blend induced by

carbon nanotubes. RSC Adv 5(123):101455–101465. https://doi.org/10.1039/C5RA20632D

Singh M, Gulamabbas T, Ahumuza B, Singh NP, Mishra V (2022) Electroactive polymeric shape memory composites for aerospace application, pp 189–210. https://doi.org/10.1002/9781119905264.ch8

Soto GD, Meiorin C, Actis D, Mendoza Zélis P, Mosiewicki MA, Marcovich NE (2018) Nanocomposites with shape memory behavior based on a segmented polyurethane and magnetic nanostructures. Polym Test 65:360–368. https://doi.org/10.1016/j.polymertesting.2017.12.012

Tang Z, Sun D, Yang D, Guo B, Zhang L, Jia D (2013) Vapor grown carbon nanofiber reinforced bio-based polyester for electroactive shape memory performance. Compos Sci Technol 75:15–21. https://doi.org/10.1016/j.compscitech.2012.11.019

Tanpitaksit T (2015) Effects of benzoxazine resin on property enhancement of shape memory epoxy: a dual function of benzoxazine resin as a curing agent and a stable network segment. Express Polym Lett 9(9):824–837. https://doi.org/10.3144/expresspolymlett.2015.77

Wang T, Farajollahi M, Choi YS, Lin IT, Marshall JE, Thompson NM, Kar-Narayan S, Madden JDW, Smoukov SK (2016) Electroactive polymers for sensing. Interface Focus 6(4):20160026. https://doi.org/10.1098/rsfs.2016.0026

Wu Y, Hu J, Han J, Zhu Y, Huang H, Li J, Tang B (2014a) Two-way shape memory polymer with "switch-spring" composition by interpenetrating polymer network. J Mater Chem A. https://doi.org/10.1039/C4TA03640A

Wu Y, Hu J, Han J, Zhu Y, Huang H, Li J, Tang B (2014b) Two-way shape memory polymer with "switch–spring" composition by interpenetrating polymer network. J Mater Chem A 2(44):18816–18822. https://doi.org/10.1039/C4TA03640A

Xia Y, He Y, Zhang F, Liu Y, Leng J (2021) A review of shape memory polymers and composites: mechanisms, materials, and applications. Adv Mater 33(6):2000713. https://doi.org/10.1002/adma.202000713

Yang H, Shi R, Jiang Q, Ren J (2022) Properties and mechanism of two-way shape memory polyurethane composite under stress-free condition. Adv Compos Hybrid Mater 6(1):1. https://doi.org/10.1007/s42114-022-00585-1

Yao Y, Zhou T, Wang J, Li Z, Lu H, Liu Y, Leng J (2016) 'Two way' shape memory composites based on electroactive polymer and thermoplastic membrane. Compos Part A Appl Sci Manuf 90:502–509. https://doi.org/10.1016/j.compositesa.2016.08.019

Zare M, Prabhakaran MP, Parvin N, Ramakrishna S (2019) Thermally-induced two-way shape memory polymers: mechanisms, structures, and applications. Chem Eng J 374:706–720. https://doi.org/10.1016/j.cej.2019.05.167

Zeng C, Liu L, Du Y, Yu M, Xin X, Liu T, Xu P, Yan Y, Zhang D, Dai W, Lan X, Zhang F, Wang L, Wan X, Bian W, Liu Y, Leng J (2023) A shape-memory deployable subsystem with a large folding ratio in China's Tianwen-1 Mars exploration mission. Engineering 28:49–57. https://doi.org/10.1016/j.eng.2023.01.005

Zhou J, Turner SA, Brosnan SM, Li Q, Carrillo J-MY, Nykypanchuk D, Gang O, Ashby VS, Dobrynin AV, Sheiko SS (2014) Shapeshifting: reversible shape memory in semicrystalline elastomers. Macromolecules 47(5):1768–1776. https://doi.org/10.1021/ma4023185

Zhou X, Zhao X, Li X, Dong J, Xu W, Zhang Q (2023) Fabrication of controllable and reversible bidirectional shape memory fabric composites based on multiblock copolyimide and their properties. Polymer 265:125608. https://doi.org/10.1016/j.polymer.2022.125608